JACC: CARDIOVASCULAR IMAGING VOL. 4, NO. 2, 2011

ISSN 1936-878X/$36.00

PUBLISHED BY ELSEVIER INC.

DOI:10.1016/j.jcmg.2010.09.022

Novel Insights Into RV Adaptation and Function in Hypoplastic Left Heart Syndrome Between the First 2 Stages of Surgical Palliation

Nee Scze Khoo, MBChB,* Jeffrey F. Smallhorn, MD,* Sachie Kaneko, MD,* Kimberly Myers, MD,* Shelby Kutty, MD,† Edythe B. Tham, MBBS*

Edmonton, Alberta, Canada; and Omaha, Nebraska

OBJECTIVES This study sought to examine the changes in ventricular function of hypoplastic left heart syndrome (HLHS) between the first 2 stages of surgical palliation.

BACKGROUND The mortality risk between first and second stages of surgical palliation in HLHS remains high. Right ventricular (RV) dysfunction predicts mortality. Postulated mechanisms include a maladaptive contraction pattern, myocardial ischemia, or contraction asynchrony. Speckle tracking imaging allows accurate measurement of myocardial deformation without geometric assumptions.

METHODS Prospective echocardiography pre-Norwood and pre-bidirectional cavopulmonary anastomosis (BCPA) examinations were performed in 20 HLHS patients, with comparisons made between stages. Measurements of ventricular function included: longitudinal/circumferential strain ratio, reflecting changes in contraction pattern; post-systolic strain index, a potential marker of myocardial ischemia; and mechanical dyssynchrony index. Relationships between echocardiographic variables and magnetic resonance imaging RV parameters before BCPA were examined.

RESULTS Before BCPA, myocardial contractility estimated by isovolumic acceleration and strain rate was reduced, paralleled by an increased in post-systolic strain index ($p < 0.01$). Right ventricular longitudinal/circumferential strain ratio decreased, becoming similar to a left ventricle–like contraction pattern, and this correlated with decreased mechanical dyssynchrony index ($r = 0.65$, $p < 0.01$), magnetic resonance imaging RV end-diastolic volume ($r = 0.65$, $p < 0.05$) and mass ($r = 0.71$, $p < 0.01$). Ventricular strain ($r = -0.72$, $p < 0.01$), strain rate ($r = -0.85$, $p < 0.001$), and mechanical dyssynchrony index ($r = -0.73$, $p < 0.01$) correlated linearly with magnetic resonance imaging–derived RV ejection fraction.

CONCLUSIONS Reduced RV contractility occurred before BCPA. RV with a left ventricle–like contraction pattern was associated with improved contraction synchrony as well as a reduction in RV size and mass in HLHS. The finding of increased post-systolic strain index before BCPA is novel and its potential link with myocardial ischemia warrants further investigation. RV strain, strain rate, and contraction synchrony measured by speckle tracking imaging correlated closely with ventricular function and might be useful for monitoring ventricular function in HLHS. (J Am Coll Cardiol Img 2011;4: 128–37) © 2011 by the American College of Cardiology Foundation

From the *University of Alberta, Stollery Children's Hospital, Edmonton, Alberta, Canada; and the †Joint Division of Pediatric Cardiology, University of Nebraska/Creighton University, Children's Hospital and Medical Center, Omaha, Nebraska. The authors have reported that they have no relationships to disclose.

Manuscript received June 29, 2010; revised manuscript received September 7, 2010, accepted September 15, 2010.

With improved surgical techniques and perioperative care, early mortality for hypoplastic left heart syndrome (HLHS) after Norwood/Sano procedure is as low as 6% (1). However, interstage mortality remains high with 2-year mortality at 19% (1). Independent risk factors for early and long-term mortality in post-HLHS palliation include tricuspid valve regurgitation (2) and right

See page 138

ventricular (RV) dysfunction (3–5). The pathophysiological processes involved in progressive RV dysfunction may include maladaptation to systemic pressure, inadequate or inappropriate hypertrophy, effects from bypass ischemia, inadequate coronary flow reserve, and dyssynchronous myocardial contraction (6–11). Despite the importance of RV dysfunction in the early stages of surgical palliation, there is a paucity of published reports studying its evolution, as conventional echocardiographic measure of the nongeometric RV function is difficult. This study investigates the usefulness of newer speckle tracking imaging (STI) in estimation of RV function in HLHS. In addition, we hypothesize that important relationships exist between RV contraction pattern (12), mechanical dyssynchrony (6), post-systolic strain index (PSSi) (a potential marker of myocardial ischemia) (13), and magnetic resonance imaging (MRI)–derived RV parameters in HLHS.

METHODS

Study population. This was a prospective study of patients with "classic" HLHS at 2 tertiary pediatric referral centers since January 2007. Variants of HLHS such as critical aortic stenosis, unbalanced atrioventricular septal defect, and heterotaxy were excluded. Patients who had completed both first and second stages of surgical repair were selected for analysis. The study was approved by the research ethics boards at both institutions.

PRE-NORWOOD CARE. Patients with prenatal diagnosis were delivered at a high-risk perinatal center, commenced on prostaglandin E_1 (0.02 μg/kg/min), and ventilated when necessary for apnea, or transportation to the tertiary institution. Acid-base status and lactate were noted at time of echocardiography. Surgical variables collected included: age at surgery, bypass time, cross clamp time, and circulatory arrest time.

PRE-BIDIRECTIONAL CAVOPULMONARY ANASTOMOSIS CARE. Patients returned at 3 and 6 months for a sedated echocardiogram using chloral hydrate (70 to 80 mg/kg). If the echocardiogram did not identify risk factors (coarctation of the aorta, pulmonary vein stenosis, restrictive interatrial communication, or significant qualitative global RV dysfunction) patients underwent cardiac MRI under general anesthesia within 30 days to assess pulmonary arteries, Norwood anastomosis, aortic arch, and RV function prior to bidirectional cavopulmonary anastomosis (BCPA).

Two-dimensional echocardiography. Standard clinical echocardiogram was performed on a Vivid 7 ultrasound machine (GE Medical Systems, Milwaukee, Wisconsin) with electrocardiogram and respiratory tracings. Additional 2-dimensional grayscale images were captured at the basal short axis and apical "4-chamber" (4CH) plane, optimized for higher frame rate (108 ± 24 Hz).

Two-dimensional echocardiography parameters analyses. Traditional parameters for assessment of RV function and size were selected from current recommendations for RV assessment in biventricular hearts (14). They included: 1) tricuspid annular plane systolic excursion (TAPSE) for longitudinal systolic RV function; 2) myocardial performance index and isovolumic acceleration (IVA) (Fig. 1), derived from color tissue Doppler imaging (TDI) assessment of annular velocities; and 3) RV fractional area change.

Measurements of ventricular function using STI analysis. Two-dimensional grayscale images were analyzed using commercially available software (EchoPAC version 7.1, GE Medical Systems) for strain and strain rate estimation. Measurements were accomplished by the following steps: 1) the systolic period was measured from onset of Q-wave to neoaortic valve closure on M-mode; 2) single cardiac loop at end expiration from basal short-axis and 4CH view was selected; 3) endocardium was traced and a speckle tracking region of interest was adjusted to fit the wall thickness; 4) the speckle tracking algorithm then divided the myocardium into 6 segments in both the basal short-axis and the 4CH view. Manual adjustments were made to ensure 2 interventric-

ABBREVIATIONS AND ACRONYMS

4CH = 4-chamber
4CH/basal strain = ratio of longitudinal/circumferential strain
BCPA = bidirectional cavopulmonary anastomosis
HLHS = hypoplastic left heart syndrome
IVA = isovolumic acceleration
LV = left ventricular
MDI = mechanical dyssynchrony index
MRI = magnetic resonance imaging
PSSi = post-systolic strain index
RV = right ventricular
STI = speckle tracking imaging
TAPSE = tricuspid annular plane systolic excursion
TDI = tissue Doppler imaging

JACC: CARDIOVASCULAR IMAGING, VOL. 4, NO. 2, 2011
FEBRUARY 2011:128–37

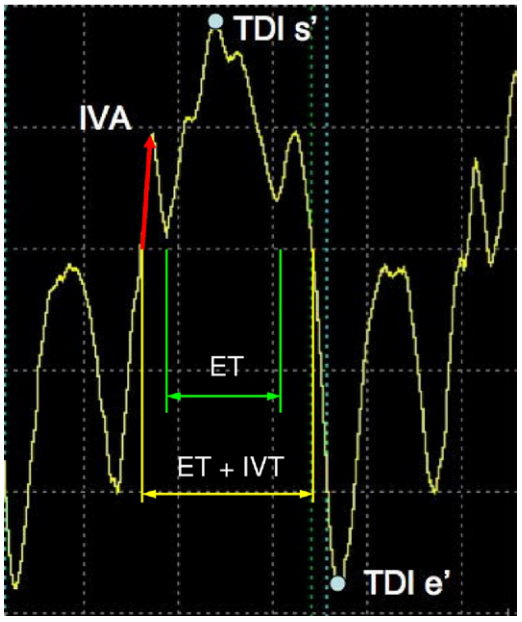

Figure 1. Velocity Curve Derived From Color TDI

Peak tissue Doppler imaging s' **(gray dot)** measures peak systolic contraction velocity. Isovolumic acceleration was measured by slope **(red arrow)**. Myocardial performance index was calculated from isovolumic time/ejection time. ET = ejection time; IVA = isovolumic acceleration; IVT = isovolumic time; TDI = tissue Doppler imaging.

ular septal segments were tracked accurately over the shortened interventricular septum (Fig. 2); and 5) strain and strain rate results over time were then displayed over time.

Derived measurements from STI. Peak strain, strain rate, and time-to-peak strain were automatically calculated from the combined deformation of the myocardial segments in each imaging plane.

Ratio of longitudinal/circumferential peak strain (4CH/basal strain) was calculated to represent the relative contribution of longitudinal and circumferential contraction to RV ejection.

Post-systolic strain index represents the fraction of strain that occurs after neoaortic valve closure. It was calculated from peak strain subtracted by peak systolic strain, divided by peak strain (Fig. 3).

Mechanical dyssynchrony index (MDI) was measured from time-to-peak strain in all 6 segments in each imaging plane normalized as a percentage of systole, with 0% at beginning of the Q-wave and 100% at neoaortic valve closure (Fig. 4). It was calculated from the standard deviation of the time-to-peak strain of the 6 segments at basal circumferential and 4CH longitudinal planes.

Cardiac MRI. Pre-BCPA cardiac MRI was performed in 12 patients under general anesthesia and free breathing using a 1.5-T scanner (Siemens Avanto, Erlangen, Germany). The median number of days between pre-BCPA echocardiography and MRI was 30 days (range 0 to 80). Prospectively gated steady state free precession cine images were acquired in contiguous short-axis locations, parallel to the tricuspid valve annulus, spanning the RVs from base to apex (echo time: 1.5 to 1.8 ms, repetition time: 3.0 to 3.6 ms, 7 views per segment, temporal resolution 20 to 25 ms, flip angle: 56°, matrix size: 192 to

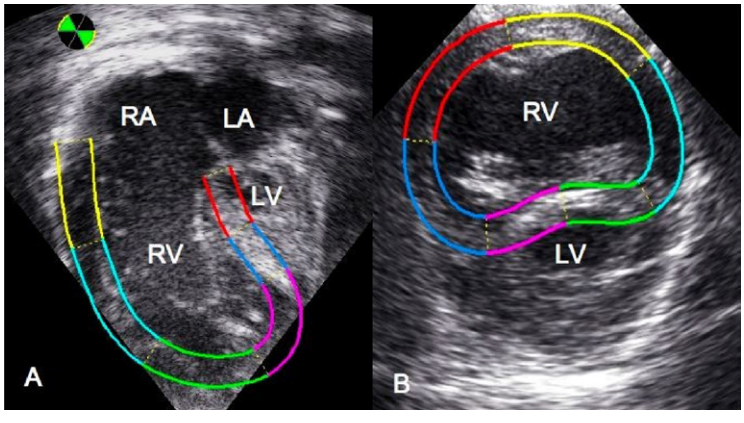

Figure 2. 4CH and Basal Short-Axis Imaging Planes With Region of Interest During STI

The 4-chamber **(A)** and basal short-axis **(B)** imaging planes with the associated manually selected region of interest during speckle tracking imaging analysis. In each imaging plane, the region of interest was divided into 6 segments, with 2 smaller segments assigned to left ventricular interventricular septum. LA = left atrium; LV = left ventricle; RA = right atrium; RV = right ventricle; STI = speckle tracking imaging; 4CH = 4-chamber.

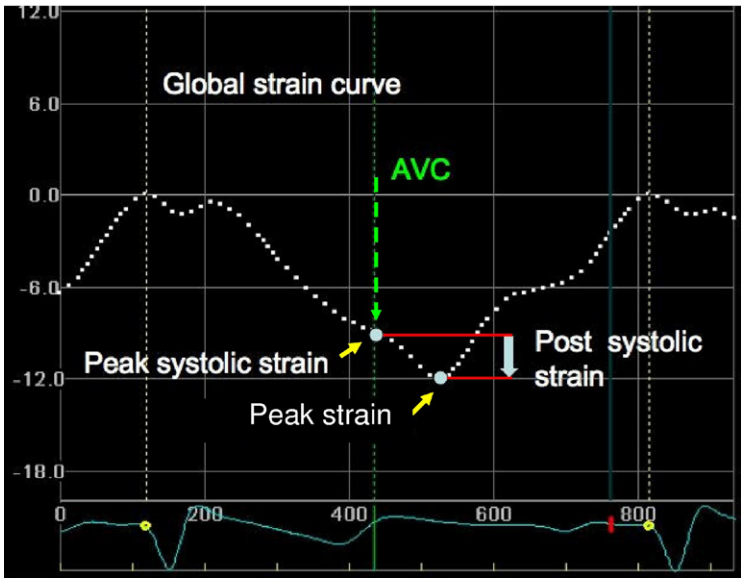

Figure 3. Strain – Time Curve Derived From STI

Strain **(y axis)** – time **(x axis)** curve derived from speckle tracking imaging analysis referenced to onset of Q-wave on electrocardiogram **(yellow dot)**. The global strain (average of the 6 segments) represented by **white dotted line.** Two **yellow arrows** indicate peak systolic strain and peak strain, respectively **(gray dots)**. Post-systolic strain was defined as strain occurring after AVC **(green dashed arrow)**, graphically represented by **broad gray arrow.** AVC = aortic valve closure; other abbreviations as in Figure 2.

256, field of view: [155 to 225] × [123 to 256] mm^2, slice thickness: 5 to 6 mm, 3 to 4 averages). Both RV end-diastolic and end-systolic volumes and RV mass were measured using offline software (Argus, Siemens) by a single observer using standard analysis methods and indexed to body

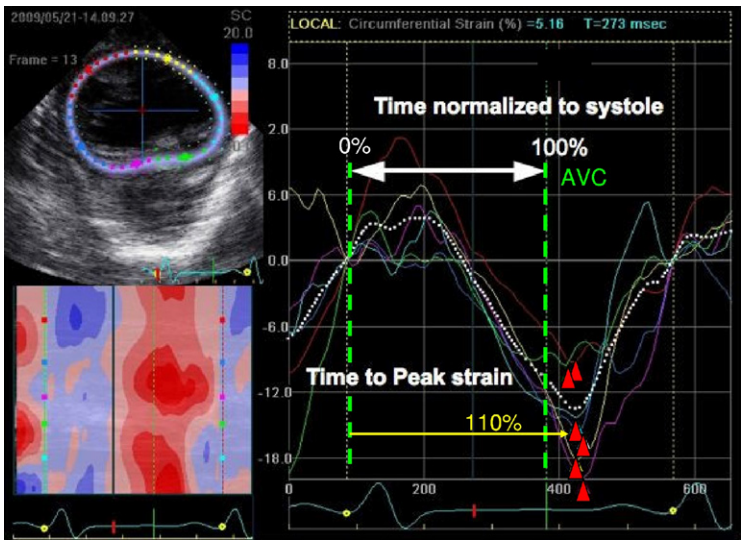

Figure 4. Color-Coded Curves Representing Strain

Six color-coded curves represent strain in each segment corresponding to color-coded segments in the short-axis 2-dimensional image **(upper left)**. All time measurements were normalized to systole with 0% at onset of Q-wave and 100% at AVC **(green dashed lines)**. **Yellow arrow** was a representative normalized time-to-peak strain. **Red triangles** indicate time at peak strain for each of the 6 segments used to calculate mechanical dyssynchrony index. Abbreviation as in Figure 3.

JACC: CARDIOVASCULAR IMAGING, VOL. 4, NO. 2, 2011
FEBRUARY 2011:128–37

Table 1. Patient Clinical Characteristics at Pre-Norwood and Pre-BCPA Assessments

Patient Variables	Pre-Norwood Median {25th, 75th Percentiles}	Pre-BCPA Median {25th, 75th Percentile}	p Value
pH	7.37 {7.32, 7.41}	—	—
Lactate	1.3 {0.9, 2.8}	—	—
Age at echocardiogram, days	3.5 {3, 7}	155 {107, 178}	—
Weight, kg	3.3 {3.1, 3.8}	5.7 {4.9, 6.7}	—
Oxygen saturation, %	88 {79, 92}	79 {75, 81}	<0.001
Systolic BP, mm Hg	62 {60, 71}	90 {81, 104}	<0.001
Diastolic BP, mm Hg	37 {30, 41}	45 {34, 50}	NS
Heart rate, beats/min	152 {149, 158}	114 {103, 126}	<0.001
ECG QRS duration, ms	86 {77, 90}	93{83,102}	NS
Tricuspid regurgitation (≥3)	3/20	4/20	—

BCPA = bidirectional cavopulmonary anastomosis; BP = blood pressure; ECG = electrocardiogram; NS = not significant.

surface area (15). The RV ejection fraction and mass/volume ratio were calculated from this data.

Statistical analysis. Results are expressed as median with {quartiles} unless otherwise stated. For comparison of continuous variables, paired Wilcoxon signed rank sum test was used. Correlations between pre-BCPA echocardiographic and MRI parameters were analyzed using Spearman correlation coefficients. Statistical significance was defined as $p < 0.05$. Interobserver variability testing was performed for peak strain, peak strain rate, time-to-peak strain, PSSi, and MDI by an independent blinded observer. Absolute differences between observers, within subject SD, repeatability (calculated as 2.77 × within subject SD), and intraclass correlation coefficients were analyzed (16,17).

RESULTS

This study consisted of 46 patients with classical HLHS who were prospectively recruited. Three patients died within 30 days of Norwood/Sano palliation (6.5%) and a further 7 died within the interstage period (15%). Sixteen patients have yet to undergo BCPA, with 20 completing BCPA palliation. Only the 20 patients who completed their first 2 stages of surgical palliation were included in our analysis.

Clinical variables. More than half the patients had a prenatal diagnosis and 65% were ventilated (Table 1). Pulse oximetry blood saturation was significantly lower at time of pre-BCPA echocardiography, 79% versus 88% before Norwood procedure ($p = 0.0002$). The proportion of patients with moderate tricuspid valve regurgitation was unchanged. Twelve-lead electrocardiographic measurement of QRS duration was not statistically different between stages. No relationship was found among Norwood surgical variables—age of surgery: 13 days {7, 16}, bypass time: 96 min {77, 158}, cross-clamp time: 46 min {35, 61} and circulatory arrest time: 24 min {19, 31}—with pre-BCPA strain, strain rate, PSSi, and MDI.

Table 2. Comparison of Traditional 2-Dimensional Echocardiographic Parameters at Pre-Norwood and Pre-BCPA Examinations

Systolic Parameters	Pre-Norwood Median {25th, 75th Quartile}	Pre-BCPA Median {25th, 75th Quartile}	p Value
MPI	0.54 {0.43, 0.68}	0.50 {0.43, 0.67}	0.50
RVFAC	0.42 {0.38, 0.47}	0.40 {0.29, 0.47}	0.37
TAPSE indexed, cm/m^2	4.0 {3.7, 4.8}	2.1 {1.7, 2.5}	<0.0001
TDI s′, cm/s	5.8 {5.3, 6.9}	3.3 {2.8, 3.8}	<0.0001
IVA/$\sqrt{}$RR	0.067 {0.045, 0.095}	0.033 {0.022, 0.053}	0.0006
RV size and geometry variables			
RVEDA indexed, cm^2/m^2	28 {23, 33}	31 {28, 37}	0.054
RVESA indexed, cm^2/m^2	16 {13, 18}	18 {16, 23}	0.11
Sphericity index	0.59 {0.53, 0.80}	0.80 {0.63, 0.91}	0.006

IVA = isovolumic acceleration; MPI = myocardial performance index; RR = R to R interval on electrocardiogram; RVEDA = right ventricle end-diastolic area; RVESA = right ventricle end-systolic area; RVFAC = right ventricle fractional area change; TAPSE = tricuspid annular plane systolic excursion; TDI = tissue Doppler imaging; other abbreviations as in Table 1.

Table 3. Comparison of STI Parameters at Pre-Norwood and Pre-BCPA Examinations

Variables	Pre-Norwood Median {25th, 75th Quartile}	Pre-BCPA Median {25th, 75th Quartile}	p Value
Basal circumferential variables			
Peak strain, %	−10.8 {−13.9, −8.5}	−13.6 {−15.2, −11.3}	NS
Peak systolic strain, %	−10.6 {−13.4, −7.6}	−10.8 {−14.8, −8.2}	NS
Time-to-peak strain, %	106 {95, 117}	114 {108, 129}	0.006
Post-systolic strain index	0.01 {0.00, 0.08}	0.08 {0.03, 0.25}	0.005
Peak strain rate, %/s	−1.26 {−1.44, −0.91}	−0.92 {−1.03, −0.78}	0.0003
Basal 6 segment MDI, %	21 {16, 32}	16 {12, 23}	0.009
4CH longitudinal variables			
Peak strain, %	−18.3 {−20.7, −16.2}	−16.2 {−18.3, −13.5}	<0.05
Peak systolic strain, %	−18.1 {−20.6, −15.9}	−14.5 {−16.5, −12.4}	0.009
Time-to-peak strain, %	101 {98, 104}	112 {106, 119}	0.0002
Post-systolic strain index	0.01 {0.00, 0.02}	0.05 {0.01, 0.12}	<0.0001
Peak strain rate, %/s	−1.63 {−2.00, −1.27}	−0.90 {−1.13, −0.76}	<0.0001
4CH 6-segment MDI, (%)	23 {15, 26}	16 {11, 18}	<0.0001
4CH/basal strain ratio	1.56 {1.47, 2.10}	1.15 {1.10, 1.40}	0.001

MDI = mechanical dyssynchrony index; STI = speckle tracking imaging; 4CH = 4-chamber; 4CH/basal strain = ratio of longitudinal/circumferential strain; other abbreviations as in Table 1.

Comparison of traditional 2-dimensional echocardiographic parameters. Pre-Norwood and pre-BCPA echocardiograms were performed at mean age of 4 days {2, 7} and 5 months {4, 6}, respectively (Table 2). Comparison of the 2 time points showed no significant difference in myocardial performance index and RV fractional area change, which are indices of global RV function. Systolic function measurements derived from longitudinal tissue velocities or deformation, such as TAPSE ($p < 0.0001$), TDI s′ at tricuspid valve annulus ($p < 0.0001$), and IVA from 4CH longitudinal color TDI ($p = 0.01$), were reduced before BCPA. An increased sphericity index before BCPA indicated a geometrical change in the RV, with increase in relative RV diameter to longitudinal length.

STI parameters. Longitudinal peak systolic strain ($p = 0.009$) was reduced before BCPA whereas circumferential peak systolic strain was unchanged (Table 3). This was reflected by a reduction in 4CH/basal peak strain ratio ($p = 0.001$) before BCPA. Pre-BCPA 4CH/basal peak strain ratio correlated positively with basal 6-segment MDI ($r = 0.64$, $p = 0.002$) but not with the 4CH 6-segment MDI ($r = 0.07$, $p = 0.77$).

We observed a delay in time-to-peak strain before BCPA (basal: 106% {95, 117} vs. 114% {108, 129}, $p = 0.006$; 4CH: 101% {98, 104} vs. 112% {106, 119}, $p = 0.0002$) and a reduction in peak strain rate (basal: $p = 0.0003$; 4CH: $p < 0.0001$), both these findings being reflected by an increase in PSSi (basal: 0.01 {0.00, 0.08} vs. 0.08 {0.03, 0.25}, $p = 0.005$; 4CH: 0.01 {0.00,

Table 4. Correlations Between Echocardiography Variables and MRI-Derived RV Parameters

	Indexed MRI-Derived RV Volumetric Parameters			
Echo Variables	RVEDV r (p Value)	RVESV r (p Value)	RVEF r (p Value)	RV Mass r (p Value)
RVEDA index	0.81 (0.001)	0.84 (0.0006)	−0.74 (0.006)	0.55 (0.06)
RVESA index	0.85 (0.0005)	0.91 (<0.0001)	−0.81 (0.001)	0.70 (0.01)
RVFAC	−0.80 (0.002)	−0.88 (0.0002)	0.81 (0.001)	−0.70 (0.01)
Basal strain	0.90 (<0.0001)	0.88 (0.0002)	−0.72 (0.008)	0.83 (0.0008)
Basal strain rate	0.82 (0.001)	0.89 (0.0001)	−0.85 (0.0005)	0.81 (0.001)
4CH strain	0.78 (0.003)	0.79 (0.002)	−0.62 (0.03)	0.62 (0.03)
4CH strain rate	0.69 (0.01)	0.71 (0.01)	−0.57 (0.053)	0.44 (0.15)
4CH/basal strain	0.65 (0.02)	0.57 (0.053)	−0.39 (0.21)	0.71 (0.01)
Basal 6-segment MDI	0.79 (0.002)	0.84 (0.0006)	−0.73 (0.007)	0.85 (0.0005)

MRI = magnetic resonance imaging; RV = right ventricular; RVEF = right ventricular ejection fraction; other abbreviations as in Tables 2 and 3.

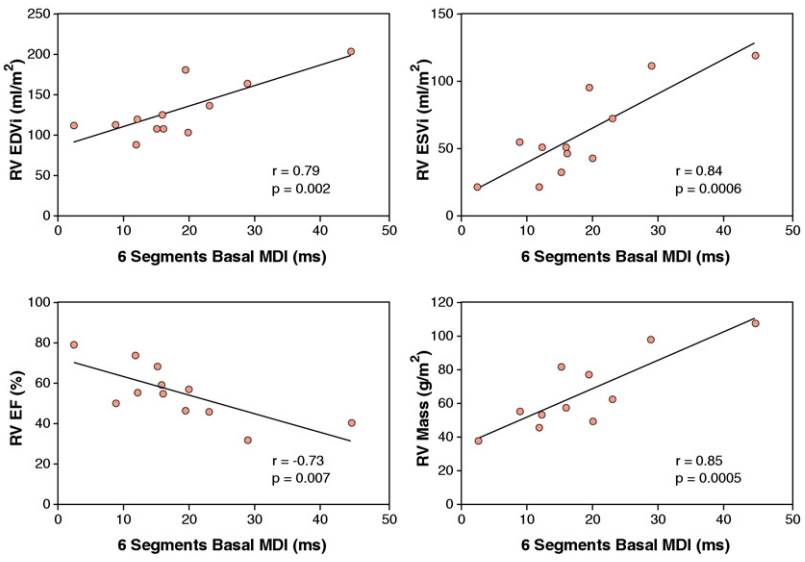

Figure 5. Basal 6-Segment MDI Correlation With Indexed MRI-Derived RV Parameters

Increasing circumferential mechanical dyssynchrony index correlated positively with increasing right ventricle size **(A, B)** and mass **(C)**, while correlating negatively with right ventricular ejection fraction **(D)**. EDVi = end-diastolic volume index; EF = ejection fraction; ESVi = end-systolic volume index; Mas = mass; MDI = mechanical dyssynchrony index; MRI = magnetic resonance imaging; other abbreviations as in Figure 2.

0.02} vs. 0.05 {0.01, 0.12}, $p < 0.0001$) before BCPA. Both MDI parameters were reduced before BCPA.

Strain and strain rate parameters correlations with MRI RV parameters. Conventional 2-dimensional echocardiographic parameters that correlated with MRI parameters were RV areas (surrogate of RV size) and the fractional area change (Table 4). Longitudinal plane displacement or velocity-derived measures of systolic function TAPSE and TDI s′ held no correlation with MRI measurements of RV volume, function, or mass, nor did RV sphericity index. IVA, a measure of cardiac contractility did not hold significant correlations with MRI RV volumes and ejection fraction. Circumferential strain and strain rate correlated closely, better than longitudinal, with MRI-derived RV volumes, function, and mass. Basal circumferential 6-segment MDI (Fig. 5) had good correlation with MRI-derived RV function. The increasing dominance of circumferential strain represented by reducing 4CH/basal strain ratio before BCPA, had linear correlations with RV end-diastolic volume index and mass (Fig. 6). No linear correlation was found between PSSi and MRI-derived RV parameters.

Interobserver variability of novel speckle tracking parameters. Novel measures for strain, strain rate, time-to-peak strain, PSSi, and MDI in the basal and 4CH planes showed minimal variability be-

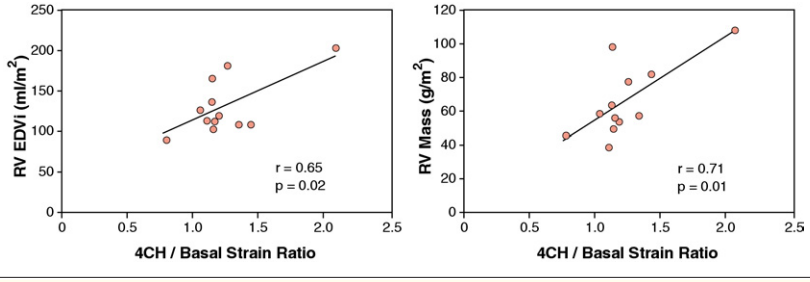

Figure 6. 4CH/Basal Strain Ratio Correlation With Indexed MRI-Derived RV Parameters

Increasing 4-chamber/basal (longitudinal/circumferential) strain ratio correlated positively with indexed right ventricular end-diastolic volume **(A)** and mass **(B)**. Abbreviations as in Figures 2 and 5.

Table 5. Interobserver Variability Testing

Variables	Absolute Difference Mean ± SD	1.96 × Within Subject SD	Repeatability	Intraclass Correlation Coefficient (r)
Basal strain, %	2.2 ± 1.5	3.7	5.3	0.80
Basal time-to-peak strain, %	4.0 ± 4.0	8.0	11.0	0.85
Basal post-systolic strain index	3.5 ± 3.6	6.8	9.7	0.91
Basal 6-segment MDI, %	4.4 ± 3.1	7.4	10.3	0.83
Basal strain rate, %/s	0.12 ± 0.09	0.21	0.28	0.84
4CH strain, %	2.0 ± 1.5	4.6	4.7	0.85
4CH time-to-peak strain, %	5.0 ± 6.0	10.0	14.0	0.78
4CH post-systolic strain index	3.1 ± 2.5	5.5	7.8	0.88
4CH 6-segment MDI, %	2.7 ± 2.4	5.0	6.9	0.75
4CH strain rate, %/s	0.14 ± 0.14	0.27	0.39	0.78

Other abbreviations as in Table 3.

tween observers (Table 5). Importantly 1.96 × within subject SD was small, a measure of the expected difference from the true value for 95% of measurements. The intraclass correlation coefficients (r = 0.75 to 0.91) were high, supporting their reproducibility. The repeatability value was also small for all novel parameters tested.

DISCUSSION

This study documents the changes in RV function between the first 2 stages of surgery for HLHS, in particular the relationship to RV size, mass, and contraction synchrony. We observed adaptation to a more left ventricle (LV)–like contraction pattern, the development of RV post-systolic strain, and the presence of RV mechanical dyssynchrony. Mechanical dyssynchrony was not only present, but also correlated with RV dysfunction.

Adaptive changes in contraction pattern. In normal biventricular hearts, shortening of the RV myocardium is greater longitudinally (18). However, when the RV is the systemic ventricle, it adopts a LV-like circumferential dominance contraction pattern (12). This was seen in our cohort by a decrease in the relative longitudinal-to-circumferential strain ratio. Furthermore, lack of adaptation to a LV-like contraction pattern was associated with an increase in mechanical dyssynchrony, ventricular dilation, and mass. Similar findings have been found in patients with idiopathic pulmonary arterial hypertension when the RV failed to adopt a LV-like contraction pattern (7). This is consistent with the current understanding of ventricular mechanics as circumferential fibers have a mechanical advantage due to myocyte contractile units being aligned along the smallest curvature of the RV free wall, allowing the most efficient generation of inward radial force (19). These changes in the RV contraction pattern are presumably an important adaptive process to maintain RV efficiency when facing chronic systemic pressures.

MDI and RV function. The presence of longitudinal contraction dyssynchrony in HLHS has been described, but not its relationship with RV function (6). Adults with varying degrees of idiopathic pulmonary arterial hypertension demonstrated RV mechanical free-wall delay, correlating strongly with RV fractional area change (20). As well, a moderate correlation of RV mechanical dyssynchrony with RV ejection fraction and predicted maximum oxygen consumption was demonstrated in the systemic RV post-atrial switch for transposition of the great arteries (21).

Our study is the first to demonstrate a significant relationship between RV mechanical dyssynchrony and MRI-derived RV function in classical HLHS. Increased basal circumferential mechanical dyssynchrony was closely associated with increased RV volume and mass, as well as ventricular dysfunction. The lack of a relationship between longitudinal mechanical dyssynchrony and RV function is consistent with previous findings in HLHS (6). This highlights the importance of measuring circumferential contraction when evaluating RV function in this population. The association of mechanical dyssynchrony with RV mass may reflect RV remodeling through compensatory hypertrophy. Literature to date, however, remains controversial as to whether an increase or decrease in RV mass/volume ratio confers survival advantage (22,23).

The pathophysiological mechanism for the unexpected finding of improved mechanical synchrony before BCPA remains unclear; however, it may be related to the cardiovascular transition from fetal to neonatal life. In those with single ventricle physiology, cardiac output would have to increase 2 to 3 times that

in fetal life to maintain adequate oxygen saturation post-natally (22). The greater degree of mechanical dyssynchrony prior to the Norwood palliation may reflect maladaptation of the single RV to early post-natal demands.

Post-systolic strain index. Increased post-systolic strain is a novel finding in the HLHS population at the pre-BPCA stage, and its significance is unclear. As post-systolic strain can occur in healthy myocardium, pathological post-systolic strain has been characterized to be transient in nature, of a larger magnitude, and a greater delay to peak strain after aortic valve closure (13). Post-systolic strain has been suggested as a marker of myocardial dysfunction resulting from ischemia (24) and myocardial contrast echocardiography demonstrated a negative correlation of post-systolic thickening with regional myocardial perfusion (25). Increased post-systolic strain in the RV has been observed during an acute increase in afterload (26). In the single LV after Fontan, increased mechanical dyssynchrony and post-systolic contraction was demonstrated using digitized angiography (27). Recently, coronary flow reserve mismatch was found in post-Fontan patients using stress positron emission tomography and implicated as a mechanism of ventricular dysfunction (10). Thus, the alterations in post-systolic strain in our HLHS population when paralleled by deterioration in RV contractility are most likely significant findings.

Conventional 2-dimensional measures of RV systolic function. Conventional 2-dimensional measures of RV function in HLHS are challenging due to the nongeometrical shape of the RV with interpretation being complicated by changes in RV volume load between staged palliations (22,28). The reduction in indexed TAPSE, TDI s′ velocity, and IVA reflect a reduction in global longitudinal systolic function between stages but provide no insight into circumferential alterations or mechanical dyssynchrony. Indeed, these traditional parameters of longitudinal function failed to account for the normal adaptation of the RV when faced with systemic pressure, and the increasingly dominant role of circumferential contraction.

Clinical implications. Our findings suggest progressive RV dysfunction in HLHS and identify several potential mechanisms important to RV function. First, it may be important for the RV to adopt a LV-like contraction pattern, which is associated with more efficient contraction mechanics. Second, circumferential mechanical synchrony is important for RV function and the prospect of resynchronization therapy for the failing RV in HLHS may be clinically relevant. The experience of early post-operative resynchronization in a mixed cohort of single ventricle patients was associated with improved cardiac output, blood pressure, and MDI (29). However, recommendations for permanent cardiac resynchronization therapy in single ventricle patients are still unclear, especially in those with RV morphology (30). Third, albeit more speculative, increased post-systolic strain may indicate that myocardial ischemia has a role in the deterioration of RV performance. This potential link may be significant and warrants further investigation.

Study limitations. Despite the relatively small sample size, the differences and correlations reported were highly significant in most and unlikely to represent a Type I error in statistics. Changes in volume load during the first 2 stages of surgical palliation for HLHS may have an impact on some echocardiographic measures of RV function performed. However, the measured indexed RV end-diastolic area, a surrogate for RV volume load, was not significantly different between stages. We also included measurements of IVA and strain rate, both of which are relatively load-independent markers of myocardial function.

CONCLUSIONS

Ventricular strain, strain rate, and mechanical synchrony using STI were reproducible and correlated closely with RV function providing a potential tool for monitoring ventricular function in HLHS. RV myocardial contractility was reduced prior to BCPA. The systemic RV showed increased dominance of circumferential contraction and this adaptation to a more LV-like contraction pattern was associated with better ventricular mechanics before BCPA. The observation of progressive increase post-systolic strain in HLHS is novel. Its potential link to myocardial ischemia is tantalizing and warrants further investigation.

Reprint requests and correspondence: Dr. Nee Scze Khoo, 8440-112 Street, 4C2 WMC, Stollery Children's Hospital, Edmonton, Alberta T6G 2B7, Canada. *E-mail: khoo@ualberta.ca.*

REFERENCES

1. Atallah J, Dinu IA, Joffe AR, et al., for the Western Canadian Complex Pediatric Therapies Follow-Up Group. Two-year survival and mental psychomotor outcomes after the Norwood procedure: an analysis of the modified Blalock-Taussig shunt and right ventricle to pulmonary artery shunt surgical eras. Circulation 2008; 118:1410–8.
2. Sano S, Huang SC, Kasahara S, Yoshizumi K, Kotani Y, Ishino K. Risk factors for mortality after the Norwood procedure using right ventricle to pulmonary artery shunt. Ann Thorac Surg 2009;87:178–86.
3. Walsh MA, McCrindle BW, Dipchand A, et al. Left ventricular morphology influences mortality after the Norwood operation. Heart 2009;95: 1238–44.
4. Gentles TL, Mayer JE, Gauvreau K, et al. Fontan operation in five hundred consecutive patients: factors influencing early and late outcome. J Thorac Cardiovasc Surg 1997;114:376–91.
5. Piran S, Veldtmann G, Siu S, Webb GD, Liu PP. Heart failure and ventricular dysfunction in patients with single or systemic right ventricles. Circulation 2002;105:1189–94.
6. Friedberg MK, Silverman NH, Dubin AM, Rosenthal DN. Right ventricular mechanical dyssynchrony in children with hypoplastic left heart syndrome. J Am Soc Echocardiogr 2007;20: 1073–9.
7. Tan JL, Prati D, Gatzoulis MA, Gibson D, Henein MY, Li W. The right ventricular response to high afterload: comparison between atrial switch procedure, congenitally corrected transposition of the great arteries, and idiopathic pulmonary arterial hypertension. Am Heart J 2007;153:681–8.
8. Penny DJ, Redington AN. Angiographic demonstration of incoordinate motion of the ventricular wall after Fontan operation. Br Heart J 1991;66: 456–9.
9. Kyriakides ZS, Athanase GM, Theofilos MK. The effects of ventricular asynchrony on myocardial perfusion. Int J Cardiol 2007;119:3–9.
10. Hauser M, Bengel FM, Kuhn A, et al. Myocardial perfusion and coronary reserve assessed by positron emission tomography in patients after Fontan-like operations. Pediatr Cardiol 2003; 24:386–92.
11. Vitarelli A, Terzano C. Do we have two hearts? New insights in right ventricular function supported by myocardial imaging echocardiography. Heart Fail Rev 2010;15:39–61.
12. Pettersen E, Helle-Valle T, Edvardsen T, et al. Contraction pattern of the systemic right ventricle. J Am Coll Cardiol 2007;49:2450–6.
13. Voigt JU, Lindenmeier G, Exner B, et al. Incidence and characteristics of segmental postsystolic longitudinal shortening in normal, acutely ischemic, and scarred myocardium. J Am Soc Echocardiogr 2003;16:415–23.
14. Lang RM, Bierig M, Devereux RB, et al., for Chamber Quantification Writing Group, American Society of Echocardiography's Guidelines and Standards Committee, European Association of Echocardiography. Recommendations for chamber quantification: a report from the American Society of Echocardiography's Guidelines and Standards Committee and the Chamber Quantification Writing Group. J Am Soc Echocardiogr 2005; 18:1440–63.
15. Hudsmith LE, Petersen SE, Francis JM, Robson MD, Neubauer S. Normal human left and right ventricular and left atrial dimensions using steady state precession magnetic resonance imaging. J Cardiovasc Magn Reson 2005;7:775–82.
16. Bland JM, Altman DG. Measurements error and correlation coefficients. BMJ 1996;313:41–2.
17. Bland JM, Altman DG. Statistic notes: measurement. BMJ 1996;313: 744.
18. Hamdan A, Thouet T, Sebastian K, et al. Regional right ventricular function and timing of contraction in healthy volunteers evaluated by strain-encoded MRI. J Magn Reson Imaging 2008;28:1379–85.
19. Ingels NB. Myocardial fiber architecture and left ventricular function. Technol Health Care 1997;5:45–52.
20. Lopez-Candales A, Dohi K, Bazaz R, Edelman K. Relation of right ventricular free wall mechanical delay to right ventricular dysfunction as determined by tissue Doppler imaging. Am J Cardiol 2005;96:602–6.
21. Chow PC, Liang XC, Lam WWM, Cheung EWY, Wong KT, Cheung YF. Mechanical right ventricular dyssynchrony in patients after atrial switch operation for transposition of the great arteries. Am J Cardiol 2008; 101:874–81.
22. Colan SD. Systolic and diastolic function of the univentricular function. Progress Pediatr Cardiol 2002;16: 79–87.
23. Sano T, Ogawa M, Taniguchi K, et al. Assessment of ventricular contractile state and function in patients with univentricular heart. Circulation 1989; 79:1247–56.
24. Asanuma T, Uranishi A, Masuda K, Ishikura F, Beppu S, Nakatani S. Assessment of myocardial ischemic memory using persistence of postsystolic thickening after recovery from ischemia. J Am Coll Cardiol Img 2009;2:1253–61.
25. Okuda K, Asanuma T, Hirano T, et al. Impact of the coronary flow reduction at rest on myocardial perfusion and functional indices derived from myocardial contrast and strain echocardiography. J Am Soc Echocardiogr 2006;19:781–7.
26. Urheim S, Abraham TP, Korinek J, Wang J, Belohlavek M. Increased right ventricular afterload induces postsystolic thickening of the ventricular septum in nonischemic hearts. J Am Soc Echocardiogr 2005;8:839–43.
27. Penny DJ, Rigby ML, Redington AN. Abnormal patterns of intraventricular flow and diastolic filling after Fontan operation: evidence for incoordinate ventricular wall motion. Br Heart J 1991;66:375–8.
28. Silverman NH, McElhinney DB. Echocardiography of hypoplastic ventricles. Ann Thorac Surg 1998;66: 627–33.
29. Bacha EA, Zimmerman FJ, Mor-Avi V, et al. Ventricular resynchronization by multisite pacing improves myocardial performance in the postoperative single-ventricle patient. Ann Thorac Surg 2004;78:1678–83.
30. Cecchin F, Frangini PA, Brown DW, et al. Cardiac resynchronization therapy (and multisite pacing) in pediatrics and congenital heart disease: five years experience in a single institution. J Cardiovasc Electrophysiol 2009;20: 58–65.

Key Words: congenital ■ echocardiography ■ heart defects ■ myocardial dyssynchrony ■ myocardial mechanics ■ myocardial strain.